

# Journal of Biomedical Optics

[SPIEDigitalLibrary.org/jbo](http://SPIEDigitalLibrary.org/jbo)

## **Absolute measurement of cerebral optical coefficients, hemoglobin concentration and oxygen saturation in old and young adults with near-infrared spectroscopy**

Bertan Hallacoglu  
Angelo Sassaroli  
Michael Wysocki  
Elizabeth Guerrero-Berroya  
Michal Schnaider Beerli  
Vahram Haroutunian  
Merav Shaul  
Irwin H. Rosenberg  
Aron M. Troen  
Sergio Fantini

# Absolute measurement of cerebral optical coefficients, hemoglobin concentration and oxygen saturation in old and young adults with near-infrared spectroscopy

Bertan Hallacoglu,<sup>a</sup> Angelo Sassaroli,<sup>a</sup> Michael Wysocki,<sup>b</sup> Elizabeth Guerrero-Berroa,<sup>b</sup> Michal Schnaider Beeri,<sup>b</sup> Vahram Haroutunian,<sup>b</sup> Merav Shaul,<sup>c</sup> Irwin H. Rosenberg,<sup>c</sup> Aron M. Troen,<sup>d</sup> and Sergio Fantini<sup>a</sup>

<sup>a</sup>Tufts University, Department of Biomedical Engineering, 4 Colby St, Medford, Massachusetts 02155

<sup>b</sup>Mount Sinai School of Medicine, One Gustave L. Levy Place, New York 10029

<sup>c</sup>Tufts University, Jean Mayer USDA Human Nutrition Research Center on Aging, Boston, Massachusetts 02111

<sup>d</sup>Hebrew University of Jerusalem, Institute of Biochemistry, Food Science and Nutrition, P.O.Box 12, Rehovot 76100, Israel

**Abstract** We present near-infrared spectroscopy measurement of absolute cerebral hemoglobin concentration and saturation in a large sample of 36 healthy elderly (mean age,  $85 \pm 6$  years) and 19 young adults (mean age,  $28 \pm 4$  years). Non-invasive measurements were obtained on the forehead using a commercially available multi-distance frequency-domain system and analyzed using a diffusion theory model for a semi-infinite, homogeneous medium with semi-infinite boundary conditions. Our study included repeat measurements, taken five months apart, on 16 elderly volunteers that demonstrate intra-subject reproducibility of the absolute measurements with cross-correlation coefficients of 0.9 for absorption coefficient ( $\mu_a$ ), oxy-hemoglobin concentration ([HbO<sub>2</sub>]), and total hemoglobin concentration ([HbT]), 0.7 for deoxy-hemoglobin concentration ([Hb]), 0.8 for hemoglobin oxygen saturation (StO<sub>2</sub>), and 0.7 for reduced scattering coefficient ( $\mu'_s$ ). We found significant differences between the two age groups. Compared to young subjects, elderly subjects had lower cerebral [HbO<sub>2</sub>], [Hb], [HbT], and StO<sub>2</sub> by  $10 \pm 4 \mu\text{M}$ ,  $4 \pm 3 \mu\text{M}$ ,  $14 \pm 5 \mu\text{M}$ , and  $6\% \pm 5\%$ , respectively. Our results demonstrate the reliability and robustness of multi-distance near-infrared spectroscopy measurements based on a homogeneous model in the human forehead on a large sample of human subjects. Absolute, non-invasive optical measurements on the brain, such as those presented here, can significantly advance the development of NIRS technology as a tool for monitoring resting/basal cerebral perfusion, hemodynamics, oxygenation, and metabolism. © 2012 Society of Photo-Optical Instrumentation Engineers (SPIE). [DOI: 10.1117/1.JBO.17.8.081406]

Keywords: biomedical optics; biophotonics; optical devices; optical properties.

Paper 120355S received Jan. 14, 2012; revised manuscript received Mar. 13, 2012; accepted for publication Mar. 22, 2012; published online May 14, 2012.

## 1 Introduction

Absolute optical measurements of bulk biological tissues are hindered by the strong diffusion of light and the spatial inhomogeneity featured by most tissues. The strong diffusion of light requires dedicated models of light propagation to characterize the absorption and scattering phenomena experienced by light in tissue. Such models include random walk analysis,<sup>1</sup> transport theory models,<sup>2</sup> and diffusion theory models.<sup>3</sup> The need to measure at least two optical coefficients to describe absorption and scattering properties of tissue is fulfilled by time-resolved approaches in the time-domain<sup>4</sup> or frequency-domain,<sup>5</sup> even though specialized continuous-wave methods have also been reported.<sup>6</sup>

Support for the validity of such methods can be obtained by absolute NIRS measurements of tissues *ex vivo*,<sup>7</sup> which allow for partial control over the shape and size of tissue and over the experimental arrangement. However, *ex vivo* optical properties are not necessarily representative of *in vivo* conditions. Absolute, non-invasive optical measurements of brain are particularly challenging because of the tissue layers (scalp, skull, dura matter, arachnoid, cerebrospinal fluid, pia matter, etc.)

that separate the optical probe from cerebral tissue. As a result, non-invasive near-infrared spectroscopy (NIRS) has typically been used to determine relative hemodynamic changes after activation in reference to basal/resting values, rather than to obtain absolute tissue concentrations of oxygen-free and oxygen-bound hemoglobin. While relative measurements may suffice for functional studies aimed at detecting hemodynamic and metabolic responses to brain activation,<sup>8–11</sup> absolute NIRS measurements can expand the scope of physiologically and clinically important information that can be acquired. Absolute NIRS measurements allow for powerful spatial mapping of resting brain cerebrovasculature, assessing changes within subjects over multiple sessions, comparing variability between subjects, and for the development of diagnostic applications requiring characterization of basal/resting brain circulation and metabolism.

Absolute NIRS studies in adult human brain report estimates of tissue oxygenation index in the range of ~65% to 75% (oxygen saturation of hemoglobin retrieved from the spectral shape of absorption coefficient);<sup>12,13</sup> cerebral venous saturation of ~70% to 75% (measured from the changes in concentrations of hemoglobin species);<sup>13,14</sup> absolute hemoglobin concentrations in the range of ~42 to 77  $\mu\text{M}$ ; and oxygen saturation of hemoglobin in cerebral tissue ranging from ~57% to 74%,

Address all correspondence to: Bertan Hallacoglu, Tufts University, Department of Biomedical Engineering, 4 Colby Street, Medford, Massachusetts 02155. Tel.+6176274359; E-mail: bertan.hallacoglu@tufts.edu

based on homogenous<sup>15–18</sup> or two-layer<sup>19,20</sup> modeling of the probed cerebral volume. Improving the accuracy, reliability, and reproducibility of absolute brain NIRS measurements is crucial to establish their utility and validity for research and clinical use, both for standalone brain oximetry and for correcting relative measurements of cerebral hemodynamics.<sup>21</sup>

Here we report results of absolute noninvasive NIRS measurements based on multi-distance, frequency-domain data that were analyzed using a diffusion theory model for a semi-infinite, homogeneous medium. We used this method to determine cerebral absorption and scattering coefficients and absolute tissue hemoglobin concentration and oxygen saturation, with a probe placed on the forehead of 55 elderly and young adult volunteers. We detected highly significant differences between the elderly and young subjects. Results of repeat measures made five months apart in a subset of 16 elderly subjects were highly reproducible. Finally, we investigated the effect of water absorption in the optical determination of tissue hemoglobin concentration and saturation.

## 2 Methods

### 2.1 Subjects

We examined fifty-five subjects of whom 36 were healthy elderly adults (mean age,  $85 \pm 6$  years; 26 females, 10 males) and 19 were young adult volunteers (mean age,  $28 \pm 4$  years; six females, 13 males). The elderly subjects were participants in an ongoing epidemiological study of aging conducted by Mount Sinai School of Medicine. Sixteen of the elderly volunteers were examined a second time five months after the first session to evaluate the reproducibility of the absolute measurements. Young adults were measured separately in a third session. Measurements in all 55 subjects were conducted in the morning or early afternoon (specifically, between the hours of 8 a.m. and 2 p.m.). The research protocol was approved by Tufts University and Mount Sinai School of Medicine Institutional Review Boards, and informed consent was obtained from all subjects prior to each measurement session. Age distribution of the subjects based on the measurement session is shown in Fig. 1.

### 2.2 Instrumentation and Data Acquisition

Measurements were performed using a multi-channel, dual-wavelength (690 and 830 nm), frequency-domain tissue oximeter (ISS Inc., Champaign, Illinois), which operates at an intensity modulation frequency of 110 MHz. The principles behind this commercially available device and the multi-distance approach have been described in detail in Ref. 22.

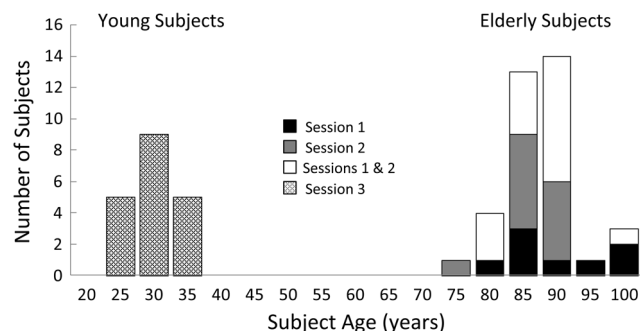


Fig. 1 Age distribution of the human subjects investigated in this study.

We employed two different polyurethane silicon optical probes featuring one collection optical fiber bundle (3 mm in core diameter) and either four or seven illumination positions each comprising two optical fibers (0.4 mm in core diameter) that guided light at 690 and 830 nm wavelengths, located several centimeters apart from the collection fiber bundles. Source-detector separations for the first probe used in session 1 were from 2 to 3.5 cm in 0.5 cm increments. Source-detector separations for the second probe used in sessions 2 and 3 were from 0.8 to 3.8 cm in 0.5 cm increments. In the elderly group, measurements were performed both on the left and the right side of the forehead close to the hair line. The probes were held in place using a commercial sports band to exert light pressure for comfort, while guaranteeing good contact between the optical fibers and the subject's skin. Because of the good agreement between left and right side measurements obtained in the elderly group, measurements in young subjects were performed only on one side (left). Figure 2 illustrates probe layout and placement.

### 2.3 Data Analysis

We used a diffusion-based, semi-infinite homogenous model to derive the absolute absorption ( $\mu_a$ ) and reduced scattering ( $\mu'_s$ ) coefficients from the frequency-domain amplitude (AC) and phase ( $\Phi$ ) values measured at multiple distances.<sup>22</sup> This model uses the following expressions:

$$\mu_a = \frac{\omega}{2\nu} \left( \frac{S_\Phi}{S_{AC}} - \frac{S_{AC}}{S_\Phi} \right), \quad (1)$$

$$\mu'_s = \frac{S_{AC}^2 - S_\Phi^2}{3\mu_a} - \mu_a, \quad (2)$$

where  $\omega$  is the angular modulation frequency of the source intensity ( $\omega = 2\pi \times 110$  MHz),  $\nu$  is the speed of light in the tissue (which is assumed here to be  $2.172 \times 10^{10}$  cm/s),  $S_{AC}$  and  $S_\Phi$ , respectively, are the slopes of  $\ln(\rho^2 \times AC)$  and  $\Phi$  as a function of source-detector separation ( $\rho$ ). Equations (1) and (2) require that light source emissions at the matching wavelengths have identical intensity and phase values. Since this is not the case (because of physical differences among the individual laser diodes, their bias and radio-frequency supplies, and their optical coupling to the tissue), we performed a calibration procedure prior to the measurements on each subject using a phantom with empirically determined optical properties that are similar to those of cerebral tissues. We determined the phantom optical properties by a calibration-free method described in Hallacoglu et al. 2011 and found to be:  $\mu_a^{690 \text{ nm}} \sim 0.19 \text{ cm}^{-1}$ ,  $\mu_a^{830 \text{ nm}} \sim 0.16 \text{ cm}^{-1}$ ,  $\mu'_s^{690 \text{ nm}} \sim 5.0 \text{ cm}^{-1}$  and  $\mu'_s^{830 \text{ nm}} \sim 4.8 \text{ cm}^{-1}$ .

We considered oxy-hemoglobin ( $\text{HbO}_2$ ), deoxy-hemoglobin (Hb) and water to be the major absorbers in the probed tissue volume at the two wavelengths considered. We did not consider other absorbers such as melanin for being present only in the thin, superficial epidermis and dermis skin layers, and lipids for their lower absorption (by a factor of 2 to 4) with respect to water absorption at the wavelengths considered by us. Under this assumption, the tissue concentrations of  $\text{HbO}_2$  and Hb can be written as follows:

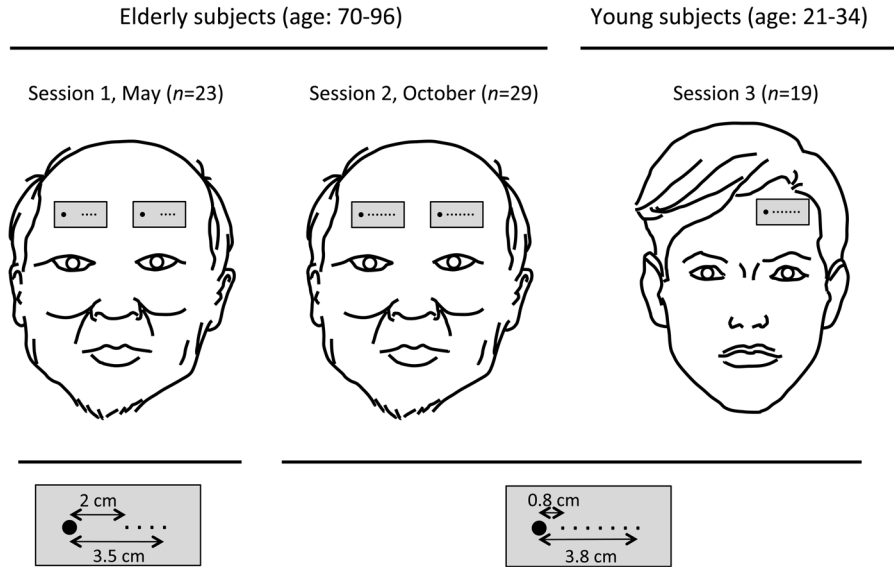


Fig. 2 Experimental setup and protocol description.

$$[\text{HbO}_2] = \frac{\mu_a^{690 \text{ nm}} \cdot \epsilon_{\text{Hb}}^{830 \text{ nm}} - \mu_a^{830 \text{ nm}} \cdot \epsilon_{\text{Hb}}^{690 \text{ nm}}}{\epsilon_{\text{HbO}_2}^{690 \text{ nm}} \epsilon_{\text{Hb}}^{830 \text{ nm}} - \epsilon_{\text{HbO}_2}^{830 \text{ nm}} \epsilon_{\text{Hb}}^{690 \text{ nm}}} - \frac{\mu_{a(\text{H}_2\text{O})}^{690 \text{ nm}} \cdot \epsilon_{\text{Hb}}^{830 \text{ nm}} - \mu_{a(\text{H}_2\text{O})}^{830 \text{ nm}} \cdot \epsilon_{\text{Hb}}^{690 \text{ nm}}}{\epsilon_{\text{HbO}_2}^{690 \text{ nm}} \epsilon_{\text{Hb}}^{830 \text{ nm}} - \epsilon_{\text{HbO}_2}^{830 \text{ nm}} \epsilon_{\text{Hb}}^{690 \text{ nm}}} C_{\text{H}_2\text{O}-\text{vf}}, \quad (3)$$

$$[\text{Hb}] = \frac{\mu_a^{830 \text{ nm}} \cdot \epsilon_{\text{HbO}_2}^{690 \text{ nm}} - \mu_a^{690 \text{ nm}} \cdot \epsilon_{\text{HbO}_2}^{830 \text{ nm}}}{\epsilon_{\text{HbO}_2}^{690 \text{ nm}} \epsilon_{\text{Hb}}^{830 \text{ nm}} - \epsilon_{\text{HbO}_2}^{830 \text{ nm}} \epsilon_{\text{Hb}}^{690 \text{ nm}}} + \frac{\mu_{a(\text{H}_2\text{O})}^{690 \text{ nm}} \cdot \epsilon_{\text{HbO}_2}^{830 \text{ nm}} - \mu_{a(\text{H}_2\text{O})}^{830 \text{ nm}} \cdot \epsilon_{\text{HbO}_2}^{690 \text{ nm}}}{\epsilon_{\text{HbO}_2}^{690 \text{ nm}} \epsilon_{\text{Hb}}^{830 \text{ nm}} - \epsilon_{\text{HbO}_2}^{830 \text{ nm}} \epsilon_{\text{Hb}}^{690 \text{ nm}}} C_{\text{H}_2\text{O}-\text{vf}}, \quad (4)$$

where  $\epsilon_{\text{Hb}}$  and  $\epsilon_{\text{HbO}_2}$  are the molar extinction coefficients of HbO<sub>2</sub> and Hb,<sup>23</sup>  $\mu_{a(\text{H}_2\text{O})}$  is the absorption coefficient of water,<sup>24</sup> and  $C_{\text{H}_2\text{O}-\text{vf}}$  is the volume fraction of water content in tissue. Equations (3) and (4) show that [HbO<sub>2</sub>] and [Hb] are linear functions of  $C_{\text{H}_2\text{O}-\text{vf}}$  with intercepts [HbO<sub>2</sub>]<sub>0</sub> and [Hb]<sub>0</sub> (corresponding to the oxy- and deoxy-hemoglobin concentrations in the absence of tissue water) and slopes that can be indicated as  $X$  and  $Y$ , respectively:

$$[\text{HbO}_2] = [\text{HbO}_2]_0 - XC_{\text{H}_2\text{O}-\text{vf}}, \quad (5)$$

$$[\text{Hb}] = [\text{Hb}]_0 + YC_{\text{H}_2\text{O}-\text{vf}}. \quad (6)$$

By using the known water absorption and hemoglobin molar extinction coefficients, for the wavelengths considered here, we find  $X = 14.9 \mu\text{M}$ , and  $Y = 1.8 \mu\text{M}$ . Total hemoglobin concentration ( $[\text{HbT}] = [\text{HbO}_2] + [\text{Hb}]$ ) and hemoglobin saturation ( $\text{StO}_2 = [\text{HbO}_2]/[\text{HbT}]$ ) are given by:

$$[\text{HbT}] = [\text{HbT}]_0 - (X - Y)C_{\text{H}_2\text{O}-\text{vf}}, \quad (7)$$

$$\text{StO}_2 = \frac{\text{StO}_2|_0 [\text{HbT}]_0 - XC_{\text{H}_2\text{O}-\text{vf}}}{[\text{HbT}]_0 - (X - Y)C_{\text{H}_2\text{O}-\text{vf}}}, \quad (8)$$

where [HbT]<sub>0</sub> and StO<sub>2</sub>|<sub>0</sub> indicate the [HbT] and StO<sub>2</sub> in the absence of water. In this study, we assumed a value of  $C_{\text{H}_2\text{O}-\text{vf}}$  of 0.7, in agreement with the choice of other optical brain studies,<sup>16,20</sup> on the basis of reported water contents of ~0.8 and ~0.7 for gray and white matters<sup>25</sup> and ~0.2 for cortical bone.<sup>26</sup>

### 3 Results

#### 3.1 Dependence on Source-Detector Distance and Reproducibility of Optical Measurements

Differences between the left and right side measurements were smaller than inter-subject variability in all parameters, and therefore we report the average of the measurements on the two sides for all elderly subjects. Young subjects were only measured on the left side (see Fig. 2).

To investigate the dependence of our measurements on source-detector separation, as a result of the layered structure of the measured tissue, we have considered subsets of data collected at three consecutive source-detector separations, spanning a range of 1 cm. By applying Eqs. (1) and (2) to such subsets of multi-distance data, we generated two sets of distance-dependent optical properties from session 1 and five sets from sessions 2 and 3 (see Fig. 2). Figure 3 shows the results of this approach for all measured parameters on elderly subjects who were measured twice (i.e., once in session 1 and once in session 2,  $n = 16$ ), where each bar represents the session mean (bar center) and standard error (bar width) over the corresponding source-detector separations (bar length). Grey and black bars in Fig. 3 represent the results obtained in session 1 and session 2, respectively. Session 2 measurements, which are richer in information content due to the greater number of source-detector distances, revealed a dependence of all parameters on source-detector distance. Results of this approach are summarized in Table 1, which compares measurements obtained from data collected at the shortest and longest sets of source-detector distances (namely, 0.8 to 1.8 cm and 2.8 to 3.8 cm), and reports their percent differences.

To assess the reproducibility of measurements, we compared source-detector distances that were common to both sessions,

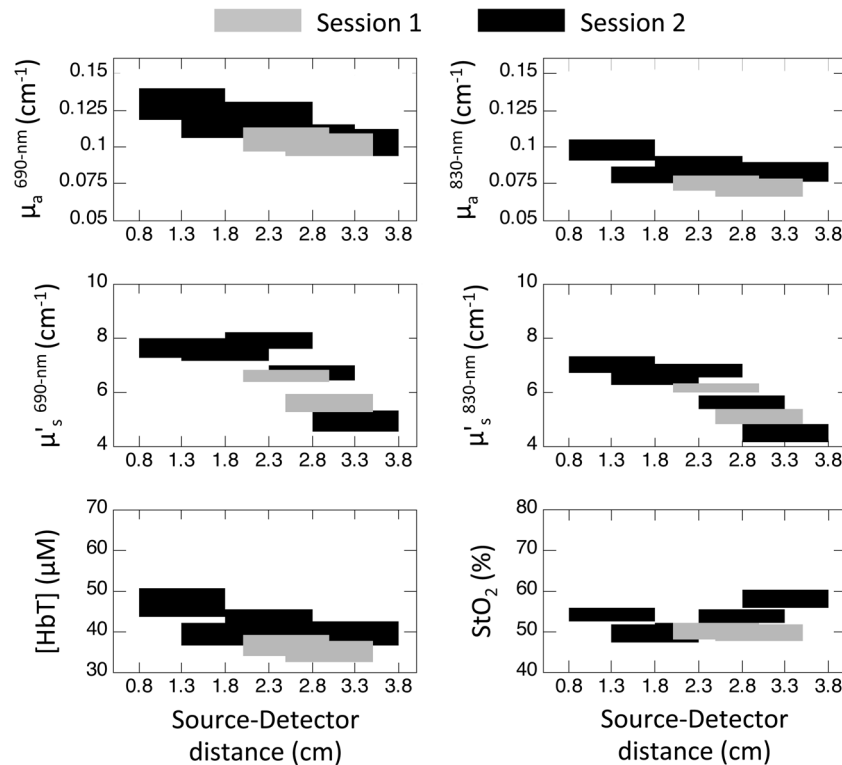


**Fig. 3** Dependence of measured parameters on source-detector separation in elderly subjects. Left and right top panels report measured  $\mu_a$  at 690 and 830 nm, respectively. Left and right middle panels report measured  $\mu'_s$  at 690 and 830 nm, respectively. Bottom left and right panels report measured [HbT] and  $StO_2$ , respectively. Grey and black blocks represent means (block center) and standard error (block thickness) of measurements in sessions 1 and 2, respectively, at corresponding distances.

namely from 2.0 to 3.5 cm in session 1 and from 2.3 to 3.3 cm in session 2. Figure 4 shows the correlation between values obtained in session 1 and 2. Good agreement was found with cross-correlation coefficients of  $\sim 0.9$  for both  $\mu_a^{690\text{ nm}}$  and  $\mu_a^{830\text{ nm}}$ ,  $\sim 0.7$  and  $\sim 0.6$  for  $\mu_s'^{690\text{ nm}}$  and  $\mu_s'^{830\text{ nm}}$ , respectively,  $\sim 0.9$  and  $\sim 0.9$  for [HbO<sub>2</sub>] and [Hb], respectively, and  $\sim 0.9$  and  $\sim 0.8$  for [HbT] and  $StO_2$ , respectively.

### 3.2 Comparison of measurements on Elderly and Young Subjects

Figure 5 shows the comparable dependence of measured parameters on source-detector distance in elderly (session 2,  $n = 29$ ) and young subjects (session 3,  $n = 19$ ), despite differences in absolute values. Grey and black bars represent the results for elderly and young subjects, respectively, over the corresponding source-detector distances (bar lengths), whereas bar centers represent means and bar widths represent standard errors. These results are also summarized in Table 1.

In order to make a meaningful comparison between physiological parameters in elderly and young subjects, we compared measurements at source-detector distances that were common to all three sessions, namely 2.0 to 3.5 cm in session 1 and 2.3 to 3.3 cm in sessions 2 and 3. We found significant differences between the two age groups in all measured parameters. We present averages and standard errors across all subjects in Fig. 6, where illustrations on the left and right sides of each graph represent measured parameters in the elderly and young subjects, respectively. These results (including [HbO<sub>2</sub>] and [Hb]) are summarized in Table 2.

## 4 Discussion

### 4.1 Multi-Distance Homogenous Model

The application of a homogeneous medium model to analyze non-invasive optical data collected on the subject's forehead is a first approximation to describe the heterogeneous composition of the probed tissue (skin, skull, brain, etc.). Our multi-distance approach over source-detector distances of 2.3 to 3.3 cm is intrinsically insensitive to the most superficial tissue layers (4 to 5 mm),<sup>27</sup> thus addressing, at least in part, the layered inhomogeneity of the investigated tissue. Nevertheless, the observed dependence of optical coefficients and hemoglobin parameters on source-detector separation (Figs. 3 and 5) implies a depth-dependence of the tissue composition, which is consistent with the head anatomy and with reports in the literature.<sup>16,19,20,28</sup> Despite this, we obtained reproducible absolute measurements in elderly subjects measured in two sessions (Figs. 3 and 4). This result is remarkable considering that the measurements were conducted five months apart with two different optical probes. Such reproducibility allows for a meaningful comparison across subjects, allowing us to observe significant differences in all measured parameters between elderly and young adults (Fig. 6). Based on the above arguments, such differences may be the result of anatomical differences, physiological differences, or a combination of them. The reproducibility of measurements of cerebral blood volume in elderly subjects based on relative NIRS measurements of hemoglobin concentration has been previously reported.<sup>29</sup> To the best of our knowledge, this is the first study showing a high level of reproducibility

**Table 1** Dependence of optical measurements on source-detector separation. Values in parentheses represent the standard error on the last significant digit(s) of the mean.

Session 2–Elderly Repeated ( $n = 16$ )	$\mu_a^{690 \text{ nm}}(\text{cm}^{-1})$	$\mu_a^{830 \text{ nm}}(\text{cm}^{-1})$	$\mu_s^{690 \text{ nm}}(\text{cm}^{-1})$	$\mu_s^{830 \text{ nm}}(\text{cm}^{-1})$	[HbO <sub>2</sub> ]( $\mu\text{M}$ )	[Hb]( $\mu\text{M}$ )	[HbT]( $\mu\text{M}$ )	StO <sub>2</sub> (%)
0.8–1.8 cm	0.13(1)	0.10(1)	7.6 (4)	7.0(3)	26(2)	22(2)	48(4)	54(2)
2.8–3.8 cm	0.10(1)	0.08(1)	4.9 (4)	4.5(4)	23(2)	17(2)	40(3)	58(2)
Percent Difference (%)	-23(10)	-20(13)	-36(6)	-36(6)	-12(10)	-23(11)	-17(9)	7(5)
Session 2–Elderly Repeated ( $n = 29$ )	$\mu_a^{690 \text{ nm}}(\text{cm}^{-1})$	$\mu_a^{830 \text{ nm}}(\text{cm}^{-1})$	$\mu_s^{690 \text{ nm}}(\text{cm}^{-1})$	$\mu_s^{830 \text{ nm}}(\text{cm}^{-1})$	[HbO <sub>2</sub> ]( $\mu\text{M}$ )	[Hb]( $\mu\text{M}$ )	[HbT]( $\mu\text{M}$ )	StO <sub>2</sub> (%)
0.8–1.8 cm	0.12(1)	0.09(1)	7.4(3)	6.8(2)	25(2)	20(1)	45(3)	55(1)
2.8–3.8 cm	0.10(1)	0.08(1)	5.7(3)	5.0(3)	21(1)	19(1)	40(2)	53(1)
Percent Difference (%)	-17(11)	-11(15)	-23(5)	-26(5)	-16(8)	-5(7)	-11(7)	-4(3)
Session 3–Young ( $n = 19$ )	$\mu_a^{690 \text{ nm}}(\text{cm}^{-1})$	$\mu_a^{830 \text{ nm}}(\text{cm}^{-1})$	$\mu_s^{690 \text{ nm}}(\text{cm}^{-1})$	$\mu_s^{830 \text{ nm}}(\text{cm}^{-1})$	[HbO <sub>2</sub> ]( $\mu\text{M}$ )	[Hb]( $\mu\text{M}$ )	[HbT]( $\mu\text{M}$ )	StO <sub>2</sub> (%)
0.8–1.8 cm	0.14(1)	0.13(1)	8.9(2)	7.5(2)	39(2)	21(1)	60(3)	64(2)
2.8–3.8 cm	0.14(1)	0.12(1)	7.2(4)	6.0(3)	39(3)	20(1)	59(4)	65(2)
Percent Difference (%)	0(10)	-8(10)	-19(5)	-20(5)	0(9)	-5(7)	-2(8)	2(4)

of absolute measurements of optical properties, hemoglobin concentration, and hemoglobin saturation in elderly subjects (Fig. 4).

#### 4.2 Measurements in Elderly Versus Young Subjects

To the best of our knowledge, this is the first study of absolute cerebral NIRS measurements of optical properties, concentrations and saturation of hemoglobin in samples of elderly and

young human subjects. Reproducibility of the results (Figs. 3 and 4) in the elderly subjects is strong evidence that measured differences between elderly and young individuals (Fig. 6) have a tissue origin. Such tissue origin, however, may be physiological (functional) and/or anatomical (structural), and the homogeneous medium model used here cannot directly discriminate between the two possibilities. Functional NIRS studies of brain activation (changes in hemoglobin concentrations and saturation) in response to cognitive challenges such as verbal fluency (rapid generation of words in a given period of time),<sup>9,30</sup> calculation,<sup>8,11</sup> and paradigm determination (arrangement and modification of pictures)<sup>10</sup> also report differences between elderly and young subjects. Even though a direct comparison between differences in changes as reported in these studies and absolute resting measurements as reported in our study is not possible, the physiological basis for these findings are expected to be related. We note also that one study has reported absolute optical properties and hemoglobin parameters on 13 subjects that implied a negative correlation between [HbO<sub>2</sub>] and subjects' ages ( $r = -0.60$ ).<sup>15</sup> It is noteworthy that we found a similar relation of [HbO<sub>2</sub>] to age ( $r = -0.58$ ), even though Gatto et al.'s study was smaller than ours (13 versus 55, respectively) and examined a narrower age range (26 to 59 versus 24 to 89). The observation of lower absolute brain tissue hemoglobin concentrations and oxygen saturation in the elderly subjects are likely to have clinical significance indicating cerebral microvascular rarefaction<sup>31</sup> or age dependent impairment in cerebral perfusion and metabolism and associated neuropathology.<sup>32</sup>

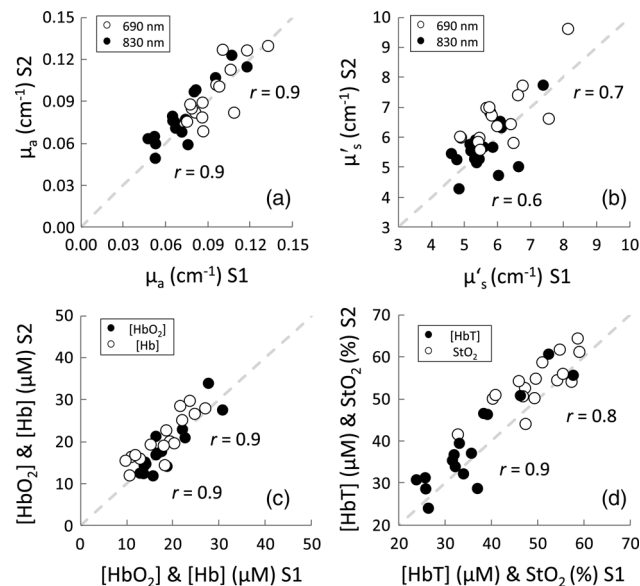


**Fig. 4** Measured parameters in session 2 as a function of corresponding parameters measured in session 1, illustrating the reproducibility of measurements taken five months apart on the same subjects. Dashed lines represent the ideal identity line to enhance reader's visualization of the data.

#### 4.3 Effect of Tissue Water Content and Calibration Procedures on the Measurement Accuracy

Water is a major tissue constituent that must be incorporated in the interpretation of optically measured hemoglobin

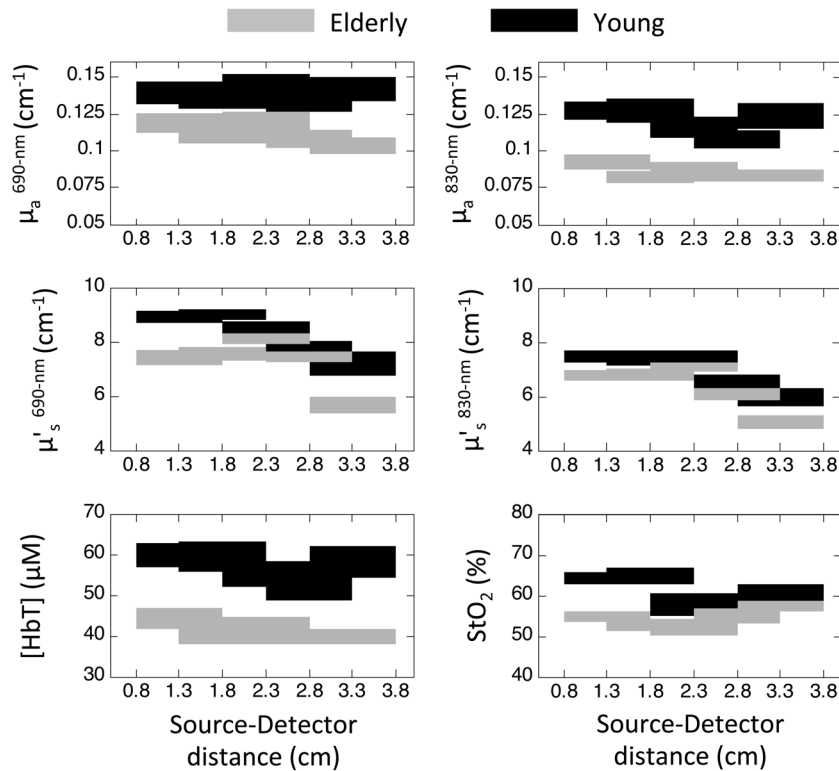


**Fig. 5** Dependence of measured parameters on source-detector separation in elderly and young subjects. Left and right top panels report measured  $\mu_a$  at 690 and 830 nm, respectively. Left and right middle panels report measured  $\mu'_s$  at 690 and 830 nm, respectively. Bottom left and right panels report measured [HbT] and  $StO_2$  respectively. Grey and black blocks represent means (block center) and standard error (block thickness) of measurements in elderly and young subjects, respectively, at corresponding distances.

concentrations. A range of values for volume fraction of water content in tissue ( $C_{H_2O-vf}$ ) have been reported in different studies, from 0.3,<sup>17</sup> to 0.7,<sup>16,20</sup> and 0.8.<sup>28,33</sup> In some cases  $C_{H_2O-vf}$  was not specified,<sup>12</sup> or was not mentioned.<sup>19</sup> Equations (5) and (6) can be used (for 690 and 830 nm wavelengths) to represent errors in [HbO<sub>2</sub>] and [Hb] due to discrepancy in considered  $C_{H_2O-vf}$  values. These equations predict that assuming no water content in the probed tissue (i.e.,  $C_{H_2O-vf} = 0$ ) results in measurements of [HbO<sub>2</sub>] that are greater than the actual values by 4.5, 10.4 and 11.9  $\mu M$ , and measurements of [Hb] that are less than the actual values by 0.6, 1.3 and 1.5  $\mu M$ , for cases in which  $C_{H_2O-vf}$  values are 0.3, 0.7 and 0.8, respectively. The relevance of taking into account the proper contribution of water absorption may, to some extent, explain differences in findings between labs and underscores the need to explicitly consider  $C_{H_2O-vf}$  in absolute NIRS measurements in cerebral tissues.

Another potential source of error is the calibration procedure. Phantom calibration for absolute NIRS measurements is a delicate protocol that requires precision in the calibration

parameters (i.e., optical properties of the phantom) to avoid errors in the estimation of hemoglobin concentrations. For our measurements, we employed an additional calibration-free protocol to measure the optical properties of the calibration phantom as described in Hallacoglu et al. 2011, which minimizes errors in the assignment of phantom optical properties to less than 5%. This in turn translates into errors of less than 4% in the measurement of tissue hemoglobin concentration.  $StO_2$  measurements, which are determined by ratios of tissue absorption at two wavelengths, are insensitive to calibration errors.

#### 4.4 General Discussion

In our recent study in a rat model of diet induced cognitive decline, we measured significantly lower absolute resting measurements of [HbT] and  $StO_2$  in cognitively impaired rats as opposed to cognitively intact controls. In addition, absolute changes in hemodynamic responses to hypoxia and hypercapnia challenges were also significantly different in the two animal

**Table 2** Summary of absolute measurements in elderly and young subjects. Values in parentheses represent the standard error on the last significant digit(s) of the mean.

	$\mu_a^{690 \text{ nm}} (\text{cm}^{-1})$	$\mu_a^{830 \text{ nm}} (\text{cm}^{-1})$	$\mu'_s{}^{690 \text{ nm}} (\text{cm}^{-1})$	$\mu'_s{}^{830 \text{ nm}} (\text{cm}^{-1})$	[HbO <sub>2</sub> ]( $\mu M$ )	[Hb]( $\mu M$ )	[HbT]( $\mu M$ )	$StO_2$ (%)
<b>Elderly</b>	0.11(1)	0.08(1)	6.9(2)	6.0(2)	20(1)	18(1)	38(2)	52(2)
<b>Young</b>	0.13(1)	0.11(1)	7.7(4)	6.6(3)	30(3)	22(2)	52(3)	58(3)

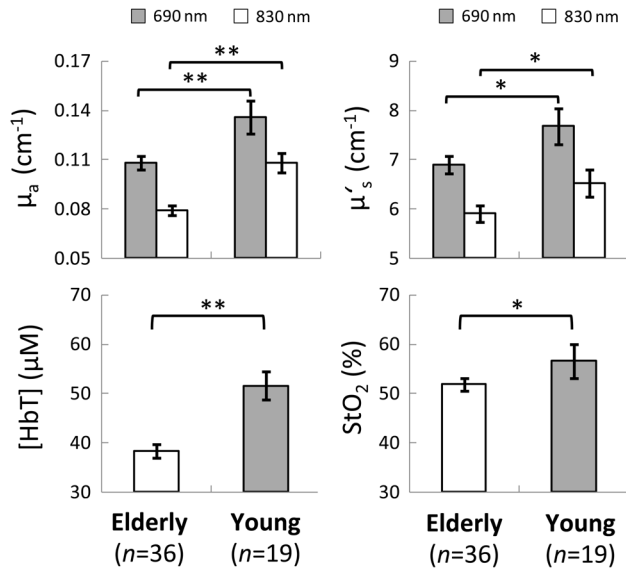


**Fig. 6** Mean and standard error of absolute measurements of optical properties, [HbO<sub>2</sub>], [Hb], [HbT], and StO<sub>2</sub> in elderly and young human subjects (\* $p < 0.05$ , \*\* $p < 0.01$ ).

groups. However when the measured changes were corrected for basal/resting values and expressed as relative measures (absolute change divided by the baseline value), the relative measures were not significantly different between the animal groups.<sup>34</sup> These findings underscore the importance of absolute NIRS measurements not only in the characterization of resting values but also in functional brain studies.

Cerebral total hemoglobin concentration and oxygen saturation values reported here in young subjects ( $52 \pm 13 \mu\text{M}$  and  $58\% \pm 9\%$ , respectively) are similar to those reported in Ref. 20 ( $51 \pm 11 \mu\text{M}$  and  $60\% \pm 4\%$ ) evaluated by a time-domain system and in Ref. 15 ( $42 \pm 13 \mu\text{M}$  and  $57\% \pm 7\%$ ), who used a frequency-domain system. Lower total hemoglobin concentration values reported in Ref. 15 may be representative of the older age group that was investigated in that study. Such hemoglobin oxygen saturation values around 60% may reflect the large oxygen consumption in the brain and/or sensitivity of non-invasive NIRS measurements to the venous compartment, whose oxygen saturation has been reported to be around 62%.<sup>35</sup> To further extend our comparison with other studies, Ohmae et al. measured comparable total hemoglobin concentration and higher oxygen saturation values ( $54 \pm 6 \mu\text{M}$  and  $70\% \pm 2\%$ ) using a time-domain system. In an independent time-domain approach, Quaresima et al. reported higher values for both total hemoglobin concentration and oxygen saturation ( $70 \pm 10 \mu\text{M}$  and  $70\% \pm 3\%$ ). Small  $C_{\text{H}_2\text{O}-\text{vf}}$  values considered in that study (0.3) relative to ours (0.7) could partially account for the greater hemoglobin concentration and oxygen saturation values. In addition, differences in probed tissue volumes between the multi-distance approach employed by us (with its suppressed sensitivity to the most superficial tissue layers) and single-distance approach by Ohmae et al. and Quaresima et al. are other plausible causes for the differences in measured hemoglobin parameters. Finally, Choi et al. reported considerably higher total hemoglobin concentration and oxygen saturation values ( $77 \pm 14 \mu\text{M}$  and  $74\% \pm 6\%$ ) using a frequency-domain instrument. Differences in the results of that study and ours may have a basis on a combination of effects including

differences in water correction (no  $C_{\text{H}_2\text{O}-\text{vf}}$  was mentioned in that study), calibration methods (optical properties of the calibration phantom was not determined independently in that study), and source-detector distances (much larger distances were used in that study  $-4.5$  to  $7$  cm).

## 5 Conclusion

Our results are among the few reported absolute optical measurements to have been made non-invasively in the human brain. Theoretically, multi-layer models might provide a more accurate measure of brain hemoglobin concentration and oxygen saturation due to the head's heterogeneous structure. However, inhomogeneous models must be able to describe the layered structure of tissue and associated boundary conditions, a task that can introduce additional errors even in the presence of complementary data and *a priori* information from independent imaging modalities. Our approach based on multi-distance measurements and a homogeneous, semi-infinite model can provide fast, reliable and robust information (as demonstrated here), while minimizing sensitivity to the most superficial tissue inhomogeneities. Such absolute measures are important because they enable physiologically meaningful comparisons of long-term changes in cerebrovascular function, both within and among subjects, and can improve relative measurements by allowing subject-specific corrections to measured changes. This represents a significant advance toward the application of NIRS to monitor long-term changes in cerebrovascular health both by stand-alone cerebral oximetry and by correcting relative measures of hemodynamic changes in functional studies.

## Acknowledgments

This research was supported by a strategic research agreement between Unilever USA and the Jean Mayer USDA Human Nutrition Research Center on Aging at Tufts, and by the U.S. Department of Agriculture, Agricultural Research Service, under agreement No. 58-1950-7-707. We also acknowledge support from NIH Grants R03-MH093846 and P01-AG02219.

The authors have no actual or potential conflicts of interest in this study.

## References

1. A. H. Gandjbakhche, H. Taitelbaum, and G. H. Weiss, "Random walk analysis of time-resolved transillumination measurements in optical imaging," *Phys. Stat. Mech. Appl.* **200**(1-4), 212-21 (1993).
2. X. Gu, K. Ren, and A. H. Hielscher, "Frequency-domain sensitivity analysis for small imaging domains using the equation of radiative transfer," *Appl. Opt.* **46**(10), 1624-1632 (2007).
3. M. S. Patterson, B. Chance, and B. C. Wilson, "Time resolved reflectance and transmittance for the non-invasive measurement of tissue optical properties," *Appl. Opt.* **28**(12), 2331-2336 (1989).
4. A. Torricelli et al., Advanced optical methods for functional brain imaging: time-domain functional near-infrared spectroscopy, in *Advances in Optical Imaging for Clinical Medicine*, pp. 287-305, John Wiley & Sons, Inc., Hoboken, NJ (2011).
5. E. Gratton et al., "Measurements of scattering and absorption changes in muscle and brain," *Philos. Trans. R. Soc. Lond. B Biol. Sci.* **352**(1354), 727-735 (1997).
6. M. Wolf, M. Ferrari, and V. Quaresima, "Progress of near-infrared spectroscopy and topography for brain and muscle clinical applications," *J. Biomed. Opt.* **12**(6), 062104 (2007).
7. W. Cheong, S. A. Prahl, and A. J. Welch, "A review of the optical properties of biological tissues," *IEEE J. Quantum Electron.* **26**(12), 2166-2185 (1990).

8. C. Hock et al., "Age dependency of changes in cerebral hemoglobin oxygenation during brain activation: a near-infrared spectroscopy study," *J. Cereb. Blood Flow. Metab.* **15**(6), 1103–1108 (1995).
9. M. Kameyama et al., "Sex and age dependencies of cerebral blood volume changes during cognitive activation: a multichannel near-infrared spectroscopy study," *Neuroimage* **22**(4), 1715–1721 (2004).
10. I. L. Kwee and T. Nakada, "Dorsolateral prefrontal lobe activation declines significantly with age—functional NIRS study," *J. Neurol.* **250**(5), 525–529 (2003).
11. M. M. Richter et al., "Brain activation in elderly people with and without dementia: influences of gender and medication," *World J. Biol. Psychiatry* **8**(1), 23–29 (2007).
12. T. S. Leung et al., "Measurement of the absolute optical properties and cerebral blood volume of the adult human head with hybrid differential and spatially resolved spectroscopy," *Phys. Med. Biol.* **51**(3), 703–717 (2006).
13. V. Quaresima et al., "Noninvasive measurement of cerebral hemoglobin oxygen saturation using two near infrared spectroscopy approaches," *J. Biomed. Opt.* **5**(2), 201–205 (2000).
14. C. Elwell et al., "Measurement of cerebral venous saturation in adults using near infrared spectroscopy," *Adv. Exp. Med. Biol.* **411**, 453–460 (1997).
15. R. Gatto et al., "Age effects on brain oxygenation during hypercapnia," *J. Biomed. Opt.* **12**(6), 062113 (2007).
16. E. Ohmae et al., "Cerebral hemodynamics evaluation by near-infrared time-resolved spectroscopy: correlation with simultaneous positron emission tomography measurements," *Neuroimage* **29**(3), 697–705 (2006).
17. V. Quaresima et al., "Bilateral prefrontal cortex oxygenation responses to a verbal fluency task: a multichannel time-resolved near-infrared topography study," *J. Biomed. Opt.* **10**(1), 11012 (2005).
18. M. Wolf et al. *Oxygen Transport to Tissue Xxiv*, J. F. Dunn and H. M. Swartz, Eds., pp. 61–73, Kluwer Academic/Plenum Publishing, New York (2003).
19. J. Choi et al., "Noninvasive determination of the optical properties of adult brain: near-infrared spectroscopy approach," *J. Biomed. Opt.* **9**(1), 221–229 (2004).
20. L. Gagnon et al., "Double-layer estimation of intra- and extracerebral hemoglobin concentration with a time-resolved system," *J. Biomed. Opt.* **13**(5), 054019 (2008).
21. C. E. Elwell and C. E. Cooper, "Making light work: illuminating the future of biomedical optics," *Philos. Trans. A Math Phys. Eng. Sci.* **369**, 4358–4379 (2011).
22. S. Fantini et al., "Frequency-domain multichannel optical detector for non-invasive tissue spectroscopy and oximetry," *Opt. Eng.* **34**(1), 32–42 (1995).
23. S. Wray et al., "Characterization of the near infrared absorption spectra of cytochrome aa3 and haemoglobin for the non-invasive monitoring of cerebral oxygenation," *Biochim. Biophys. Acta* **933**(1), 184–192 (1988).
24. G. M. Hale and M. R. Querry, "Optical constants of water in the 200-nm to 200-microm wavelength region," *Appl. Opt.* **12**(3), 555–563 (1973).
25. H. Q. Woodard and D. R. White, "The composition of body tissues," *Br. J. Radiol.* **59**(708), 1209–1218 (1986).
26. A. Techawiboonwong et al., "Cortical bone water: in vivo quantification with ultrashort echo-time MR imaging," *Radiology* **248**(3), 824–833 (2008).
27. M. A. Franceschini et al., "Influence of a superficial layer in the quantitative spectroscopic study of strongly scattering media," *Appl. Opt.* **37**(37), 7447–7458 (1998).
28. D. Comelli et al., "In vivo time-resolved reflectance spectroscopy of the human forehead," *Appl. Opt.* **46**(10), 1717–1725 (2007).
29. J. A. Claassen, W. N. Colier, and R. W. Jansen, "Reproducibility of cerebral blood volume measurements by near infrared spectroscopy in 16 healthy elderly subjects," *Physiol. Meas.* **27**(3), 255–264 (2006).
30. M. J. Herrmann et al., "Cerebral oxygenation changes in the prefrontal cortex: effects of age and gender," *Neurobiol. Aging* **27**(6), 888–894 (2006).
31. W. R. Brown and C. R. Thore, "Review: cerebral microvascular pathology in ageing and neurodegeneration," *Neuropathol. Appl. Neurobiol.* **37**(1), 56–74 (2011).
32. C. Iadecola, "The overlap between neurodegenerative and vascular factors in the pathogenesis of dementia," *Acta Neuropathol.* **120**(3), 287–296 (2010).
33. A. Torricelli et al., "In vivo optical characterization of human tissues from 610 to 1010 nm by time-resolved reflectance spectroscopy," *Phys. Med. Biol.* **46**(8), 2227–2237 (2001).
34. Hallacoglu et al., "Cerebral perfusion and oxygenation are impaired by folate deficiency in rat: absolute measurements with noninvasive near-infrared spectroscopy," *J. Cereb. Blood Flow Metab.* **31**(6), 1482–1492 (2011).
35. E. L. Gibbs et al., "Arterial and cerebral venous blood. Arterial differences in man," *J. Biol. Chem.* **144**(2), 325–332 (1942).